

# Higher-Order Singularities without Glass-Glass Transitions

— *An Avoided Glass-Glass Transition* —

Matthias SPERL<sup>\*)</sup>

*Institut für Materialphysik im Weltraum,  
Deutsches Zentrum für Luft- und Raumfahrt,  
51170 Köln, Germany*

Within the framework of mode-coupling theory, the glass-transition scenario is investigated for a system of particles interacting with a hard-core repulsion and an additional square-shoulder soft core at larger distances. The static structure is calculated from the potential in Percus-Yevick approximation. For certain widths of the shoulder, the exponent parameter  $\lambda$  along the glass-transition line shows a double peak. At both peaks,  $\lambda$  can reach unity indicating the existence of higher-order glass-transition singularities. It is shown that these higher-order singularities originate from a line of avoided glass-glass transitions.

## §1. Introduction

In the field of glassy slow dynamics, many experiments and simulations have been inspired in recent years by the mode-coupling theory for idealized glass transitions (MCT).<sup>1)</sup> Within this theory, the transition from a liquid to an idealized glass state is described by a bifurcation in the solutions of certain polynomials in a variable  $f$ : Upon smooth variations of a control parameter, say, the temperature  $T$ , variable  $f$  jumps from  $f = 0$  to a finite critical value  $f = f^c > 0$  at  $T = T_c$  and increases further with the distance from the transition  $T_c - T$ . Variable  $f$  is defined by the long-time limit of some autocorrelation function  $\phi(t)$ ; states with  $f > 0$  are identified as glass states, while states with  $f = 0$  shall be called fluid or ergodic.

The mentioned bifurcations originate from the equations of motion for density autocorrelation functions  $\phi_q(t)$  of a system of  $N$  particles in a volume  $V$  with density  $\rho = N/V$ . The time-dependent fluctuations in the density are used to define the canonical normalized correlation function  $\phi_q(t) = \langle \rho(t)^* \rho \rangle / \langle \rho^* \rho \rangle$  as is well-known in liquid-state theory.<sup>2)</sup> In this case, the correlation functions depend on the wave vector modulus  $q$  of the corresponding Fourier transform in space. Using projection-operator techniques, one can derive the following equations of motion

$$\partial_t^2 \phi_q(t) + \nu_q \partial_t \phi_q(t) + \Omega_q^2 \phi_q(t) + \Omega_q^2 \int dt' m_q(t-t') \partial_{t'} \phi_q(t') = 0, \quad (1.1a)$$

with characteristic frequencies  $\Omega_q$ , a white noise  $\nu_q$ , and the memory function

$$m_q(t) = \mathcal{F}[\phi_k(t), V] = \frac{1}{2} \int \frac{d^3 k}{(2\pi)^3} V_{\vec{q}, \vec{k}} \phi_k(t) \phi_{|\vec{q}-\vec{k}|}(t), \quad (1.1b)$$

---

<sup>\*)</sup> E-mail: matthias.sperl@dlr.de

where the interaction potential is encoded in the vertex

$$V_{\vec{q},\vec{k}} = \rho S_q S_k S_{\vec{q},\vec{k}} \rho \left[ \vec{q}\vec{k}c_k + \vec{q}(\vec{q} - \vec{k})c_{|\vec{q}-\vec{k}|} \right]^2 / q^4, \quad (1.1c)$$

through the static structure factor  $S_q$  of the fluid and  $c_q$  its direct correlation function. Both functions can be calculated from the interaction potential together with some closure relation that is known typically only in some approximation.<sup>2)</sup> For  $t \rightarrow \infty$ , one gets an algebraic equation for the correlators' long time limits  $\phi_q(t) \rightarrow f_q$ ,

$$\frac{f_q}{1 - f_q} = \mathcal{F}[f_k, V]. \quad (1.1d)$$

It was discovered in 1984 that Eq. (1.1d) can exhibit nontrivial solutions,  $f_q > 0$ , for microscopic interaction potentials and realistic values of the density in the system.<sup>3)</sup> It was shown later that only singularities of type  $A_\ell$  can occur in Eq. (1.1d),<sup>4)</sup> and these singularities are equivalent to those emerging for the parameter space of roots of polynomials upon variation of the coefficients.<sup>5)</sup> Hence, an  $A_2$  singularity – also called *fold* – signals a double root in the solutions like in the equation  $x^2 + t = 0$  for  $t_c = 0$ . For a polynomial of high enough order, the variation of a single control parameter is sufficient to encounter an  $A_2$  singularity. Generically, the variation of  $\ell - 1$  control parameters is necessary to identify singularities of type  $A_\ell$ . An  $A_3$  singularity – called *cusp* – requires two control parameters to adjust a polynomial to a cubic root; an  $A_4$  singularity – the *swallowtail* – requires the variation of three parameters. It was shown in a theorem by Whitney that only  $A_2$  and  $A_3$  are robust singularities, all other singularities can be removed by small perturbations of the control parameters.<sup>5), 6)</sup>

Within MCT, the  $A_2$  singularity can be identified with a liquid-glass transition if  $f$  jumps from  $f = 0$  to a finite value  $f^c$  at the transition. Once such a singularity is identified, asymptotic expansions of Eq. (1.1) can be used to derive the long-time behavior of the correlator  $\phi(t)$ . For the  $A_2$  singularity, these asymptotic expansions yield two-step relaxation, time-temperature superposition, and power-law scaling.<sup>1)</sup> The unique number characterizing the leading terms of the asymptotic expansion for an  $A_2$  singularity is the exponent parameter  $\lambda$  which is between 0.5 and unity. In addition to liquid-glass transitions, fold singularities can also describe glass-glass transitions: In this case an existing first glass state with  $f \geq f_1^c$  transforms into a second distinct glass state with  $f \geq f_2^c > f_1^c$  discontinuously. The endpoint of a line of glass-glass transition points is the  $A_3$  singularity. An  $A_4$  singularity signals the emergence of a glass-glass transition line from an otherwise smooth surface of liquid-glass transitions. Every  $A_\ell$  singularity is characterized by a unique number  $\mu_\ell \geq 0$  that determines the properties of the asymptotic expansions.<sup>7)</sup>  $\mu_\ell \rightarrow 0$  signals the emergence of the higher-order singularity  $A_{\ell+1}$  where in turn  $\mu_{\ell+1}$  defines the leading terms of the expansion. An  $A_2$  singularity's exponent parameter is identical to  $\mu_2 = 1 - \lambda$ . Therefore, a fold gives rise to a cusp once  $\lambda$  approaches unity.

## §2. Glass Transitions, Glass-Glass Transitions, and Higher-Order Singularities

In the following, the transition singularities of MCT shall be reviewed briefly for hard spheres (sec. 2.1), sticky hard spheres (sec. 2.2), and the square-well potential (sec. 2.3). The section 2 shall be concluded with the discussion of newly discovered transitions in the square-shoulder system (sec. 2.4) where the static structure factors are evaluated in Roger-Young (RY) approximation. In sec. 3, new results shall be given for the square-shoulder system with the static structure factors calculated from the Percus-Yevick (PY) approximation. The comparison between results from RY- and PY-calculations gives insight into the robustness of the predicted glass-glass transition phenomena.

### 2.1. Glass Transition for the Hard-Sphere System – a Fold

MCT was first applied to the hard-sphere system (HSS) where a glass transition was identified upon varying the control parameter packing fraction  $\varphi = \pi\rho d^3/6$  for particles of hard-sphere diameter  $d$ .<sup>3)</sup> The transition is predicted for a packing fraction of  $\varphi^c = 0.516$  when using the PY approximation for the calculation of the static structure factor  $S_q$ .<sup>2)</sup> The hard-sphere interaction can be realized to a very good degree in experiments performed in colloidal suspensions. In such experiments the glass transition is found around a packing fraction  $\varphi^c = 0.58$ , moreover, the two-step relaxation, scaling laws and several other features of the theoretical predictions are confirmed.<sup>8)</sup> From a thorough analysis of Eq. (1.1c) one can derive that for the HSS, the glass transition is driven by the hard-core repulsion as encoded in the principal peak of the static structure factor. The HSS has been investigated by asymptotic expansions<sup>9)</sup> with the exponent parameter being around  $\lambda = 0.7$  which is close to the typical value for many other glass forming substances. The full evolution of glassy dynamics over eight orders of magnitude in time for various densities has been demonstrated for a tagged particle's mean-squared displacement (MSD).<sup>10)</sup>

### 2.2. Glass-Glass Transition in the Sticky Hard-Sphere System – a Cusp

For the investigation of an  $A_3$  singularity, more than one control parameter needs to be varied. Generically the variation of two control parameters extends an isolated  $A_2$  singularity to a line of  $A_2$  singularities, so the existence of an  $A_3$  singularity is by no means certain. However, if such an  $A_3$  singularity exists in the given parameter plane, it can be found as an endpoint of a line of  $A_2$  singularities where close to the  $A_3$ , these  $A_2$  singularities can be identified as glass-glass transition points. At the  $A_3$ , the distinction between the different glass states, the discontinuity between the  $f_q$  on both sides of the glass-glass transition, vanishes. Such endpoint singularities have been described first for so-called schematic models of MCT where the microscopic details, i.e., the  $q$ -dependence, has been dropped in favor of mathematical simplicity. Rather than a precise interaction potential these models capture the mathematical structure of the problem. In these schematic models the transition points can be calculated analytically and the asymptotic expansions are not affected by limited numerical accuracy. For such schematic models, the asymptotic expan-

sions for singularities  $A_\ell$  with  $\ell > 2$  have been performed: Two-step relaxation and time-temperature superposition become invalid, and – most notably – logarithmic decay laws emerge.<sup>7),11)</sup>

The first microscopic model with an  $A_3$  singularity in its parameter plane was found for Baxter’s sticky hard-sphere model (SHSS).<sup>12)</sup> The SHSS adds a short-ranged attraction to the hard-sphere potential similar to the square-well interaction, cf. Fig. 1 (a). However, within the SHSS, depth  $\Gamma$  and width  $\delta$  can only be changed together while the product  $\Gamma\delta$  remains fixed, in addition the limit  $\delta \rightarrow 0$  is performed; this defines a so-called stickiness parameter  $\tau$ . Hence, the SHSS has two control parameters, packing fraction  $\varphi$  like the HSS and the stickiness  $\tau$ . For the SHSS, the MCT predicts glass-glass transitions and an  $A_3$  endpoint singularity.<sup>13),14)</sup> The glass-glass transitions take place between a repulsion-dominated glass state – as known from the HSS – and an attraction-dominated glass state that resembles bond formation as known from the gelation transition.<sup>14)</sup> While for a treatment of the SHSS within MCT, a cutoff wave-vector space needs to be introduced, it is by now well-known how this cutoff can be interpreted as an inverse length scale, and how the MCT results stay well-defined.<sup>15)</sup> In accordance with Whitney’s theorem, for small changes in the cutoff neither fold nor cusp singularities change qualitatively.

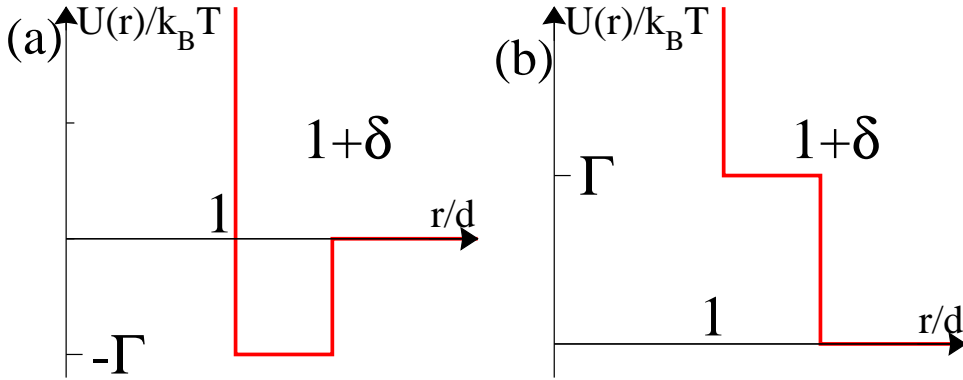


Fig. 1. (a) Square-well potential with three control parameters: packing fraction  $\varphi = \pi\rho d^3/6$ , well depth  $\Gamma = u_0/k_B T$ , and well width  $\delta$  for particles of diameter  $d$  at density  $\rho$ . (b) Square-shoulder potential with shoulder height  $\Gamma = u_0/k_B T$  and shoulder width  $\delta$ .

### 2.3. Glass-Glass Transitions in the Square-Well System – a Swallowtail

In order to avoid entirely the introduction of a cutoff and other peculiarities of the SHSS, one can extend the model attraction to finite widths in the square-well system (SWS), cf. Fig. 1 (a). Here, the control-parameter space becomes truly three dimensional, the parameter triple  $(\varphi, \Gamma, \delta)$  defines each state. The MCT glass-transition scenarios have been worked out for the SWS,<sup>16)</sup> and in addition to the cusp scenario of the SHSS there exists a characteristic well width  $\delta^*$  for the SWS above which no cusp singularity can be found in the  $(\varphi, \Gamma, \bar{\delta})$  parameter plane for fixed  $\bar{\delta}$  when  $\bar{\delta} > \delta^*$ . When  $\bar{\delta} < \delta^*$ , the SWS always exhibits a glass-glass transition line with an  $A_3$  singularity as endpoint. For the exceptional point  $\delta = \delta^*$ ,

the glass-glass transition lines together with the line of  $A_3$  singularities vanish in an  $A_4$  singularity, giving rise to a three-dimensional geometric structure known as swallowtail. In contrast to the stable  $A_2$  and  $A_3$  singularities, the  $A_4$  is an isolated point in the parameter space that is sensitive to small numerical deviations from  $(\varphi^*, \Gamma^*, \delta^*)$ . But while the details of the approximations involved and the numerical implementation change the location of the  $A_4$  singularity, its existence is a robust prediction of MCT for systems with short-ranged attraction regardless of the specific interaction model<sup>15)</sup> or closure relation for the static structure factors.<sup>16)</sup>

The occurrence of the glass-glass transitions can be traced to two different mechanisms of arrest – resulting from the interplay of repulsion and attraction – in the vertex, cf. Eq.(1.1c). The repulsion-dominated glass state within MCT is produced by the local structure on the wave-vector scale of the peak of  $S_q$ . The second mechanism of arrest is given by a  $1/q$ -tail in  $S_q$  for large wave vectors  $q$ .<sup>16)</sup> Once that tail has enough weight in the vertex, a second transition – the glass-glass transition – can occur. This possibility of an additional transition is robust regarding the closure relation as long as the tail can become large enough. This independence of the results from the closure relation was demonstrated explicitly for the PY compared with the mean-spherical approximation.<sup>16), 17)</sup>

The asymptotic solutions have been worked out in detail for the SWS and involve logarithmic decay laws,<sup>18)</sup> Vogel-Fulcher-like divergence of time-scales,<sup>19)</sup> unconventional (i.e., non-power-law) critical decays at the higher-order singularities,<sup>20)</sup> and the interplay of two  $A_2$  singularities at the crossing of glass- and gel-transition lines.<sup>17)</sup> Experimental verifications of the scenarios predicted for the SWS are found in computer simulations and in colloidal suspensions with attraction among the particles. Confirmations include the reentrant behavior of the lines of  $A_2$  singularities,<sup>21)–23)</sup> the dynamics at a crossing of glass- and gel-transition lines for micellar<sup>24), 25)</sup> and colloidal suspensions,<sup>26)</sup> and the logarithmic decay of correlation functions together with novel power laws for the MSD.<sup>18), 27)</sup>

#### 2.4. Glass-Glass Transitions in the Square-Shoulder System

When the attractive well of the SWS is replaced by a repulsive step, one obtains the square-shoulder system (SSS), cf. Fig. 1 (b). The SSS also has three control parameters,  $(\varphi, \Gamma, \delta)$ , with  $\Gamma$  now symbolizing the height of a shoulder. Allowing the control parameter  $\Gamma$  to carry a sign, SWS and SSS may even be plotted into a single diagram. Recently, the MCT predictions for the SSS have been worked out using the RY approximation<sup>28)</sup> for  $S_q$ .<sup>29)</sup> Further details and references to the numerical algorithms can be found in recent work.<sup>29)</sup>

Figure 2 shows the results of MCT for the SSS at  $\delta = 0.145$ : For  $\Gamma = 0$ , the glass transition line (lower panel) emerges from the HSS value of  $\varphi_{\text{HSS}}^{\text{RY}} = 0.5206$ , increases in density until around  $\Gamma = 3$ , bends over in an S-shape towards the HSS limit for the outer core,  $\varphi = 0.5206/(1+0.145)^3 = 0.3468$ . The form of the transition curve can be understood in detail from the distortions of the local structures by the presence of the repulsion at distance  $1 + \delta$  and the resulting changes to the principal peak of the static structure factor.<sup>29)</sup> For both reentrant transitions it can be shown how the weakening of the local structure is compensated by either higher density (in

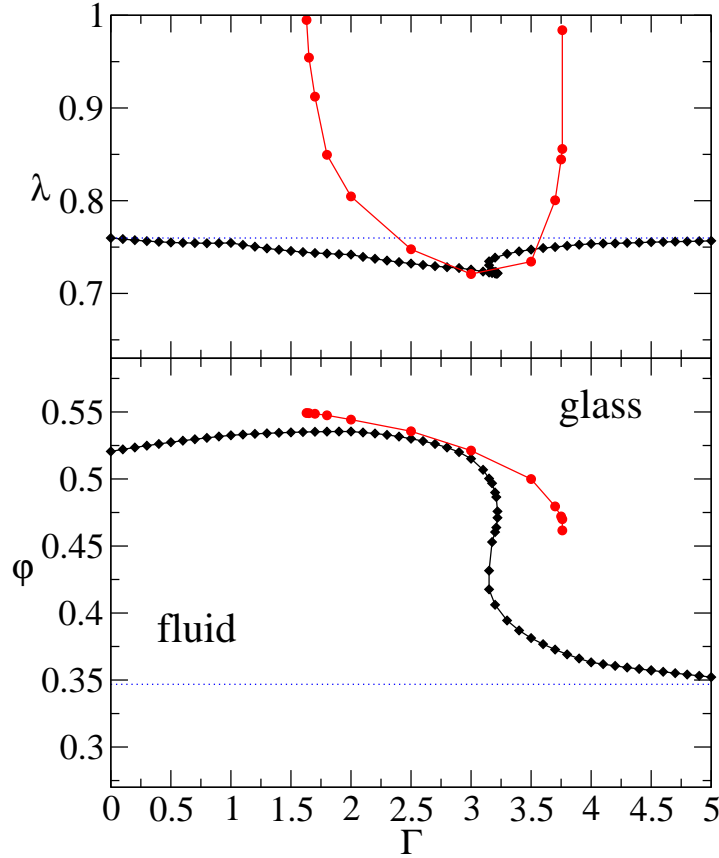


Fig. 2. Glass-transition diagram (lower panel) and exponent parameter  $\lambda$  for the SSS using the RY approximation at  $\delta = 0.145$ . Diamonds show the transition points from an ergodic state to a glass state; filled circles exhibit the glass-glass transition points. Dotted lines show the limits for the hard-sphere system with diameter  $1 + \delta$ .

the case of melting by cooling, i.e., melting at increasing  $\Gamma$ ) or lower temperature which is equivalent to higher  $\Gamma$  (in the case of melting by compression). In the pressure-temperature representation, such a reentrant behavior can be identified with a so-called diffusion anomaly which is known experimentally e.g. for water.<sup>30)</sup> The exponent parameter  $\lambda$  (upper panel) varies very little along the glass-transition line and stays around the common value of  $\lambda = 0.7$ . From this unremarkable value for  $\lambda$  no conclusion can be drawn about any glass-glass transitions or higher-order singularities in the vicinity.

Moving further into the glass state,  $f_q$  experiences an additional jump marked by the full circles in Fig. 2. In contrast to the situation for the SWS, for the SSS the glass-glass-transition line is located completely within the glassy state. This gives rise to two endpoints, two  $A_3$  singularities. These two endpoints are seen also in the upper panel of Fig. 2 where  $\lambda$  approaches unity on either side. This novel line originates from the competition of the two repulsive cores that causes a beating in the static structure factor for large wave vectors; this beating – if sufficiently large in

amplitude – can bring additional weight to the MCT vertex in Eq. (1.1c) and hence cause an additional discontinuous transition.<sup>29)</sup> In physical terms, the localization of the already arrested particles drops drastically when the glass-glass transition line is crossed since upon crossing the line, the localization now happens at the outer core rather than at the inner core as before. When varying the control parameters, the beating is most pronounced when inner and outer core have about the same impact on  $S_q$  – if either one of the cores is dominant, the beating is diminished and the discontinuous transition ends in two  $A_3$  singularities, respectively. Physically, the glass-glass transition becomes impossible at the upper endpoint when the density becomes too high for a transition to the outer core; the glass-glass transition also vanishes at the lower endpoint because the density becomes too low at the respective shoulder height to force the particles closer together. For shoulder widths  $\delta$  larger than the value shown in Fig. 2, the glass-glass transition line moves towards and merges with the glass-transition line.<sup>29)</sup>

### §3. Square-Shoulder System using the Percus-Yevick Approximation

In this section, it is demonstrated how the scenario shown in sec. 2.4 changes when the mentioned beating has not enough weight in the vertex (1.1c) to cause an additional transition line.

Figure 3 shows the glass-transition scenarios for various shoulder widths of the SSS when the PY approximation is used for the calculation of the static structure factor. The overall behavior of the transition diagram is similar to the RY results: The glass-transition first increases in packing fraction  $\varphi$  when starting from the HSS limit  $\varphi_{\text{HSS}} = 0.516$  at  $\Gamma = 0$ . Around  $\Gamma = 2.5$  the curve bends downwards and reaches the limit of the HSS with an outer core of  $\varphi_{\text{HSS}}/(1 + \delta)^3$  at around  $\Gamma = 5$ . Different from the RY result, the S-shape of the transition curve for intermediate values of  $\Gamma$  only develops at higher values for the width  $\delta$ . Also in contrast to the RY result, there appears to be no indication of additional discontinuities in the  $f_q$  or endpoint singularities inside the glass regime. However, while  $\lambda$  in the upper panel of Fig. 2 stays almost constant at the glass-transition line for the RY results, for the glass-transition line within PY approximation the exponent parameter  $\lambda$  varies considerably with  $\Gamma$  for any given width  $\delta$  in the upper panel of Fig. 3. In addition, the shape of the  $\lambda$ -versus- $\Gamma$  curves varies drastically with  $\delta$ . For  $\delta = 0.25$ , an exponent-parameter maximum is around  $\lambda = 0.85$  which is already rather high. For larger  $\delta$ , the  $\lambda$ -versus- $\Gamma$  curves exhibit double maxima over relatively small intervals in  $\Gamma$ , like between 1.85 and 2.1 for  $\delta$  around 0.28. For  $\delta = 0.2785$  and  $\delta = 0.28$  the parameter  $\lambda$  approaches unity very closely at the right and the left end of the interval, respectively. Beyond that regime,  $\lambda$  decreases again for larger  $\delta$ , and as shown for  $\delta = 0.3$ , the separation of both  $\lambda$  maxima increases; the  $\lambda$  maxima are located at  $\Gamma = 1.65$  and  $\Gamma = 2.4$ , respectively, while their values are still as high as 0.9. In summary, while no glass-glass line can be detected, the exponent parameter approaches  $\lambda = 1$  very closely. These results indicate a nearby higher-order singularity without the presence of glass-glass transitions. More puzzling still is the existence of two maxima in  $\lambda$  very close to each other.

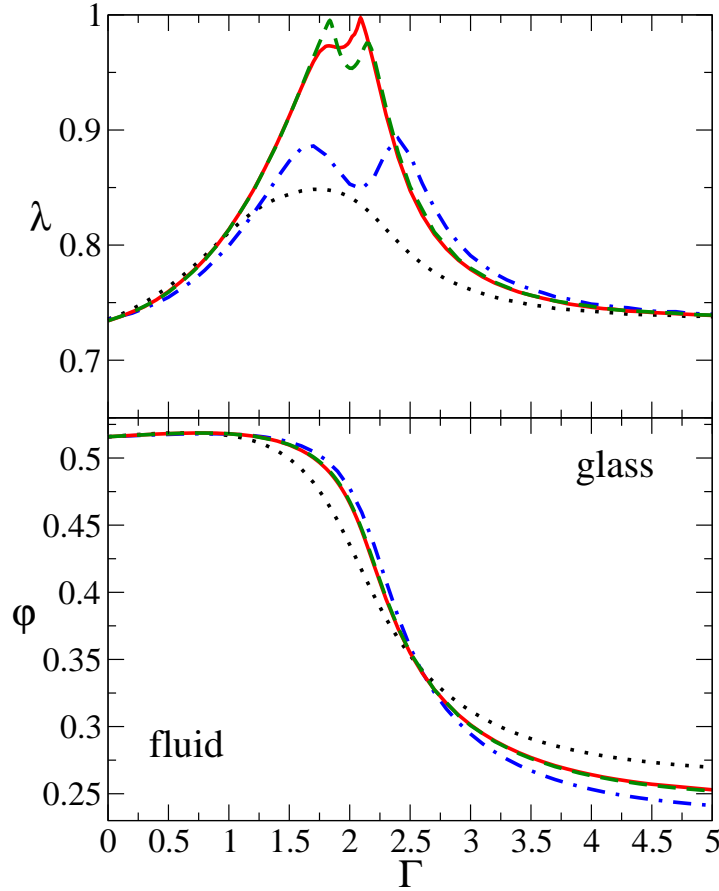


Fig. 3. Glass-transition scenario (transition lines in the lower and exponent parameter  $\lambda$  in the upper one) for the SSS using the PY approximation for  $\delta = 0.25$  (dotted line), 0.2785 (full line), 0.28 (dashed line), and 0.3 (chain line). In the lower panel, the curves for  $\delta = 0.2785$  and 0.28 are almost on top of each other.

To clarify the nature of the higher-order singularities on the glass-transition curves, the glassy region is inspected in more detail for  $\delta = 0.25$  in Fig. 4. The behavior of  $\lambda$  indicates that here the higher-order singularities are further away from the transition line, but a rather broad maximum already hints at these. It is well-known that after crossing an  $A_2$  glass-transition singularity, the long-time limits  $f_q$  increase above their critical value  $f_q^c$  in a square-root in the control parameter; i.e. in the HSS, this increase is proportional to  $\sqrt{\varphi - \varphi_{\text{HSS}}^c}$ .<sup>9)</sup> When a glass-glass transition occurs, this square-root increase after the first transition is superseded by an additional discontinuity in  $f_q$  followed by the square-root increase after this second transition. While this additional discontinuity was used to identify the glass-glass transition line in Fig. 2, such discontinuity is absent for the PY calculations. Nevertheless, the evolution of the  $f_q$  within PY approximation shows a characteristic deviation from the square-root behavior in certain parameter regions: First, the range of validity of the square-root increase is sometimes far smaller than known from



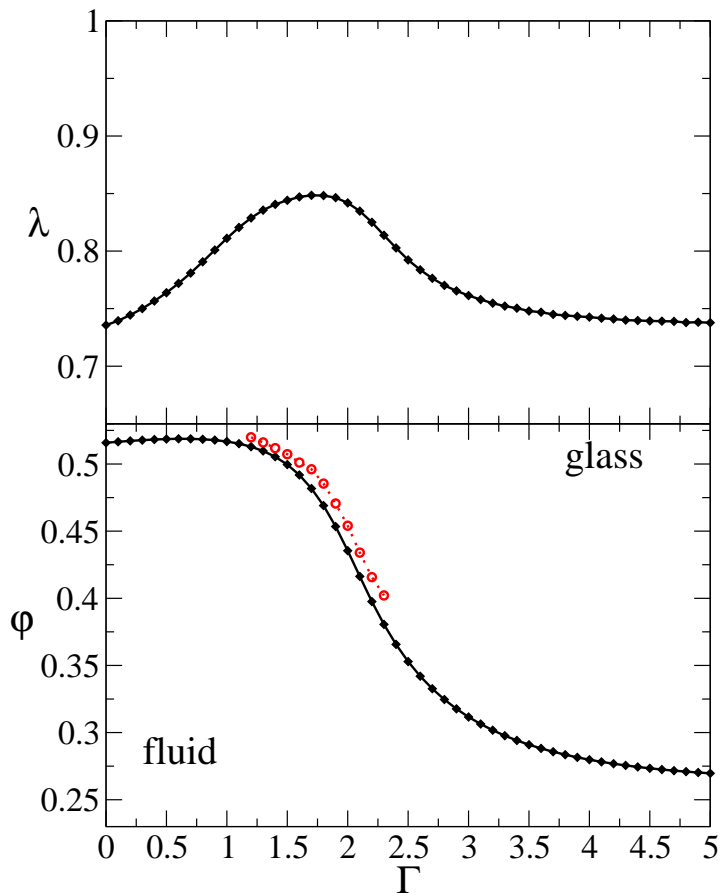


Fig. 4. Glass-transition scenario for the SSS for  $\delta = 0.25$ . Diamonds show the  $A_2$  singularities at glass-transition points. The open circles mark the position of an anomaly in the evolution of the  $f_q$ , see text – a line of hidden glass-glass transition points emerges.

the HSS; second, the apparent square-root increase at larger distances from the glass-transition indicates a square-root with a different extrapolated transition point  $\varphi^{\text{app}}$  than the one given by the discontinuity in  $f_q$  at  $\varphi^c$ . This difference between the actual and the apparent transition point can be quantified as a difference in the control parameters, say as a relative difference in packing fraction,  $\Delta\varphi = (\varphi^{\text{app}} - \varphi^c)/\varphi^c$ . When this relative difference in packing fraction exceeds 1%, this anomaly is marked by open circles in Fig. 4. It is seen that this line of  $f_q$  anomalies strongly resembles the line of glass-glass transitions in Fig. 2. It can therefore be concluded that within MCT both approximations, PY and RY, yield similar glass-transition scenarios with a possible line of glass-glass transitions inside the glassy regime.

#### §4. Conclusion

In the present work, the glass-transition diagram for the SSS has been calculated for the PY approximation. These results can now be used to estimate the robust-

ness of the results for the SSS obtained with a different closure relation, e.g. with results from the RY approximation.<sup>29)</sup> While the comparison of different closure relations for the SWS only resulted in shifts of the control parameters, the situation is more involved in the case of the SSS. The existence of the disconnected glass-glass transition line depends on two trends that both become more prominent for larger values of  $\delta$ . First, the vertex in Eq. (1.1c) obtains additional weight for higher wave vectors through a beating phenomenon as described above; this makes a glass-glass transition possible if the weight becomes strong enough. Second, at the same time this supposed glass-glass transition line moves closer to the glass transition line and merges with it. For the RY approximation, the glass-glass transition line becomes manifest through a discontinuity in  $f_q$  and then moves towards the glass transition line. In contrast for the PY approximation, the not-yet-manifest glass-glass transition moves towards the glass transition line and merges with it before it is fully developed as a discontinuity in the  $f_q$ . When the endpoints of this hidden line of glass-glass transitions merge with the regular glass transition line, very high values of  $\lambda$  result since the first trend of increased weight for a glass-glass transition keeps increasing. In this sense, the glass-glass transition line emerges extremely close and on top of the glass transition line and is at the same moment absorbed by the glass transition line.

The differences between RY and PY approximation with respect to the higher-order singularities and the corresponding glass-glass transitions are highly non-trivial in the theoretical calculations. However, for the experimental test if such a scenario exists, both scenarios need to be observed in combination: Numerical deviations similar to the ones shifting the HSS-PY transition from  $\varphi^c = 0.516$  to 0.58 in the experiment can for the SSS switch from the RY scenario shown earlier<sup>29)</sup> to the PY scenario described here.

### Acknowledgments

This work was partially supported by Yukawa International Program for Quark-Hadron Sciences (YIPQS). Support from BMWi under 50WM0741 is gratefully acknowledged. I want to thank W. Götze, J. Horbach, P. Kumar, F. Sciortino H. E. Stanley and E. Zaccarelli for fruitful collaboration and discussion of the work.

### References

- 1) Wolfgang Götze. *Complex Dynamics of Glass-Forming Liquids: A Mode-Coupling Theory*. Oxford University Press, Oxford, 2009.
- 2) J.-P. Hansen and I. R. McDonald. *Theory of Simple Liquids*. Academic, London, 2nd edition, 1986.
- 3) U. Bengtzelius, W. Götze, and A. Sjölander. Dynamics of supercooled liquids and the glass transition. *J. Phys. C*, 17:5915–5934, 1984.
- 4) W. Götze and L. Sjögren. General properties of certain non-linear integro-differential equations. *J. Math. Analysis and Appl.*, 195:230–250, 1995.
- 5) V. I. Arnol'd. *Catastrophe Theory*. Springer, Berlin, 3rd edition, 1992.
- 6) Hassler Whitney. On singularities of mappings of euclidean spaces. i. mappings of the plane into the plane. *Annals of Mathematics*, 62:374–410, 1955.
- 7) W. Götze and M. Sperl. Logarithmic relaxation in glass-forming systems. *Phys. Rev. E*, 66:011405, 2002.

- 8) W. van Megen and P. N. Pusey. Dynamic light-scattering study of the glass transition in a colloidal suspension. *Phys. Rev. A*, 43:5429–5441, 1991.
- 9) T. Franosch, M. Fuchs, W. Götze, M. R. Mayr, and A. P. Singh. Asymptotic laws and preasymptotic correction formulas for the relaxation near glass-transition singularities. *Phys. Rev. E*, 55:7153–7176, 1997.
- 10) M. Sperl. Nearly-logarithmic decay in the colloidal hard-sphere system. *Phys. Rev. E*, 71:060401, 2005.
- 11) W. Götze and L. Sjögren. Logarithmic decay laws in glassy systems. *J. Phys.: Condens. Matter*, 1:4203–4222, 1989.
- 12) R. J. Baxter. Percus-yevick equation for hard spheres with surface adhesion. *J. Chem. Phys.*, 49:2770–2774, 1968.
- 13) L. Fabbian, W. Götze, F. Sciortino, P. Tartaglia, and F. Thiery. Ideal glass-glass transitions and logarithmic decay of correlations in a simple system. *Phys. Rev. E*, 59:R1347–R1350, 1999.
- 14) J. Bergenholtz and M. Fuchs. Non-ergodicity transitions in colloidal suspensions with attractive interactions. *Phys. Rev. E*, 59:5706–5715, 1999.
- 15) W. Götze and M. Sperl. Higher-order glass-transition singularities in systems with short-ranged attractive potentials. *J. Phys.: Condens. Matter*, 15:S869–S879, 2003.
- 16) K. Dawson, G. Foffi, M. Fuchs, W. Götze, F. Sciortino, M. Sperl, P. Tartaglia, Th. Voigtmann, and E. Zaccarelli. Higher-order glass-transition singularities in colloidal systems with attractive interactions. *Phys. Rev. E*, 63:011401, 2001.
- 17) M. Sperl. Dynamics in colloidal liquids near a crossing of glass- and gel-transition lines. *Phys. Rev. E*, 69:011401, 2004.
- 18) M. Sperl. Logarithmic relaxation in a colloidal system. *Phys. Rev. E*, 68:031405, 2003.
- 19) M. Sperl. Logarithmic decay in a two-component model. In M. Tokuyama and I. Oppenheim, editors, *Slow Dynamics in Complex Systems*, volume 708 of *AIP Conference Proceedings*, pages 559–564, New York, 2004. AIP.
- 20) W. Götze and M. Sperl. Critical decay at higher-order glass-transition singularities. *J. Phys.: Condens. Matter*, 16:S4807–S4830, 2004.
- 21) T. Eckert and E. Bartsch. Re-entrant glass transition in a colloid-polymer mixture with depletion attractions. *Phys. Rev. Lett.*, 89:125701, 2002.
- 22) G. Foffi, K. A. Dawson, S. V. Buldyrev, F. Sciortino, E. Zaccarelli, and P. Tartaglia. Evidence for unusual dynamical arrest scenario in short ranged colloidal systems. *Phys. Rev. E*, 65:050802, 2002.
- 23) K. N. Pham, A. M. Puertas, J. Bergenholtz, S. U. Egelhaaf, A. Moussaïd, P. N. Pusey, A. B. Schofield, M. E. Cates, M. Fuchs, and W. C. K. Poon. Multiple glassy states in a simple model system. *Science*, 296:104–106, 2002.
- 24) W.-R. Chen, S.-H. Chen, and F. Mallamace. Small-angle neutron scattering study of the temperature-dependent attractive interaction in dense l64 copolymer micellar solutions and its relation to kinetic glass transition. *Phys. Rev. E*, 66:021403, 2002.
- 25) S.-H. Chen, W.-R. Chen, and F. Mallamace. The glass-to-glass transition and its end point in a copolymer micellar system. *Science*, 300:619–622, 2003.
- 26) K. N. Pham, S. U. Egelhaaf, P. N. Pusey, and W. C. K. Poon. Glasses in hard spheres with short-range attraction. *Phys. Rev. E*, 69:011503, 2004.
- 27) F. Sciortino, P. Tartaglia, and E. Zaccarelli. Evidence of a higher-order singularity in dense short-ranged attractive colloids. *Phys. Rev. Lett.*, 91:268301, 2003.
- 28) F. J. Rogers and D. A. Young. New, thermodynamically consistent, integral equation for simple fluids. *Phys. Rev. A*, 30:999–1007, 1984.
- 29) M. Sperl, E. Zaccarelli, F. Sciortino, P. Kumar, and H. E. Stanley. Disconnected glass-glass transitions and diffusion anomalies in a model with two repulsive length scales. submitted, arXiv:0910.3673, 2009.
- 30) C. A. Angell, E. D. Finch, and P. Bach. Spinecho diffusion coefficients of water to 2380 bar and 2c. *J. Chem. Phys.*, 65:3063, 1976.